




Sintered electrode full cells for high energy density lithium-ion batteries

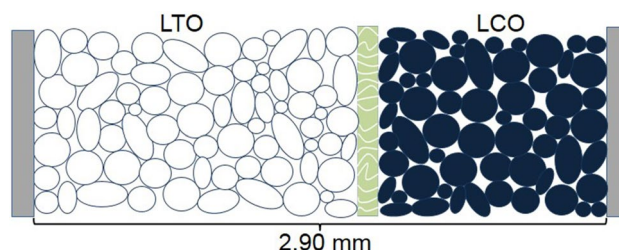
J. Pierce Robinson¹ · John J. Ruppert¹ · Hongxu Dong¹ · Gary M. Koenig Jr.¹ 

Received: 15 March 2018 / Accepted: 6 August 2018 / Published online: 10 August 2018
© Springer Nature B.V. 2018

Abstract

Increasing the energy density of lithium-ion batteries at the electrode and cell level is necessary to continue the reductions in the size and weight of battery cells and packs. Energy density improvements can be accomplished through increasing active material density in electrodes by decreasing porosity and removing inactive additives, as well as by using thicker electrodes that reduce the relative fraction of separators and current collectors in the cell. This paper describes the fabrication of sintered electrodes comprised of only electro-active material toward the goal of thick electrodes free of binders and conductive additives. The electrodes reported herein have no inactive additives in the electrode, > 62% active material volume fraction, and high thicknesses of > 500 μm . The high capacity of these electrodes presents challenges for material characterization and extended cycling. In particular, lithium metal anodes limit the performance of sintered electrode cells at > 1 mA cm^{-2} , a relatively low rate for these thick electrodes. In this work, full $\text{Li}_4\text{Ti}_5\text{O}_{12}/\text{LiCoO}_2$ (LTO/LCO) sintered electrode cells with total combined thickness of anode, separator, and cathode of up to 2.90 mm have been successfully fabricated and electrochemically evaluated. These full cells have improved stability and high areal capacities, as high as 45 mAh cm^{-2} capacity at 1.28 mA cm^{-2} .

Graphical abstract



Keywords Lithium-ion battery · All active material electrode · Thick electrode · Energy storage

Electronic supplementary material The online version of this article (<https://doi.org/10.1007/s10800-018-1242-y>) contains supplementary material, which is available to authorized users.

✉ Gary M. Koenig Jr.
gary.koenig@virginia.edu

¹ Department of Chemical Engineering, University of Virginia, 102 Engineers Way, Charlottesville, VA 22904-4741, USA

1 Introduction

Continued growth in the number of battery-powered devices such as portable electronics and electric vehicles demands the development of higher energy density batteries, with lithium-ion (Li-ion) batteries still the dominant choice for these rechargeable applications [1]. While development of new Li-ion materials chemistry is one approach to increase cell energy density [2, 3], substantial improvements in energy density can also be achieved by using established materials through improved engineering of the battery electrodes [4,

5]. In particular, higher energy density electrodes can be accomplished by increasing the volume fraction of active material via higher packing densities, removing inactive additives, and/or increasing electrode thicknesses.

Designing electrodes for high total energy or energy density often results in compromises in the rate capability of the electrode. Removal of conductive additives and binders in composite electrodes will reduce the electrode electronic conductivity and mechanical integrity, respectively [6, 7]. Calendaring is a process often done to improve electronic conductivity and increase the volumetric energy density of a composite electrode, but this step reduces the volume of the electrode allocated to the electrolyte, creating restrictions in Li^+ transport [8, 9]. Also, thick and dense electrodes can be difficult to manufacture without cracking or delamination [10]. Large particles, which pack well into composite electrodes, have longer internal diffusion paths and lower surface areas for intercalation reactions which limits rate capability of the battery cell [11, 12]. The combination of the factors described above leads to common processing and design limits for composite electrodes, and most composite electrodes reported for Li-ion batteries have thicknesses below 250 μm and active material volume fractions below 60% [2, 13, 14].

This manuscript will describe battery cells where both the anode and cathode are comprised of sintered electrodes that contain only the electroactive materials, a less common electrode architecture for Li-ion batteries [4]. These sintered electrodes consist of close-packed solid active material particles (> 60% solid by volume) compressed into porous thin films. These thin films are electronically conductive, and thus do not require conductive additives. In addition, the connections between particles are mechanically robust and thus binders are also not required, thus the sintered electrodes do not have any of the inactive additives typically used in conventional Li-ion composite electrodes. Using hydraulic pressing to fabricate the electrodes enables thicker electrodes than those typically achieved with calendared composites. The pressing of a single component, the active material particles, mitigates some electrode heterogeneity. Furthermore, the pressing step achieves random close packing regardless of particle morphology, facilitating the use of small, high-rate-capability active material particles without major sacrifices to electrode packing density [15]. Sintered electrodes have higher energy densities on an areal basis than state-of-the-art composite electrodes [16], and the increased thickness of the electrodes suggests that if they could be produced in a stacked configuration that due to the lower fraction of the cell allocated to separators and current collectors that sintered electrodes may even be competitive with wound composite electrode architectures [17].

Herein, fabrication of Li-ion full cells will be reported where both electrodes were comprised of only sintered

active materials—free of binder and conductive additives. The coin cells reported in this study have extremely high areal capacities—21.4 mAh cm^{-2} and 45.2 mAh cm^{-2} . For perspective, commercial Li-ion electrode pairs have been reported in a range generally up to 25 mg active material per cm^2 , corresponding to a capacity of about 3.75 mAh cm^{-2} for common cathode material LiCoO_2 (LCO) [2, 18]. While other reports have paired sintered electrodes with lithium metal which results in the highest energy density, this report will demonstrate that lithium metal thin film electrodes result in significant performance and cycle life limitations when paired with high capacity sintered electrode cells. The high energy density sintered electrode architectures provide a promising route to high energy density Li-ion cells, and further improvements toward mitigating rate capability limitations in these cells would provide a promising strategy to designing high energy density battery packs.

2 Results and discussion

2.1 Sintered electrode half cells

LCO was chosen for evaluation toward use as the cathode in sintered electrode full cells, in part because it was previously demonstrated in the literature as a successful sintered electrode material [4]. LCO is a good candidate for use as a sintered electrode material because it has reasonably high energy density, relatively high electronic conductivity after slight delithiation, and modest strain with intercalation/deintercalation [4, 19]. Relatively high electronic conductivity is important for sintered electrodes because the active material itself must provide all of the electronic conduction from the particles to the current collector, and as will be described in the cell fabrication, some of the active material particles in the electrode will be many hundreds of micrometers away from the current collector. Modest intercalation strain is needed because large volume change in the electrode material with cycling would likely lead to fracture and failure of the electrode because it is comprised of only sintered active material. Strain of more than a few percent would be expected to break particle–particle sintered connections.

LCO powder was synthesized as described in “[Experimental](#)” section, pressed into 440 μm thick pellets (surface morphology can be seen in Fig. S1 in Supplementary Material), sintered, and assembled into half cells with lithium metal anodes to evaluate the electrochemical performance. For comparison with the Li/LCO sintered electrodes, Li/LCO cells were also fabricated using conventional LCO composite electrodes where the composite was comprised of a blend of active material, carbon black, and binder with relative weight fractions of 80:10:10 active material:carbon black:binder. As shown in Fig. 1, the sintered electrodes

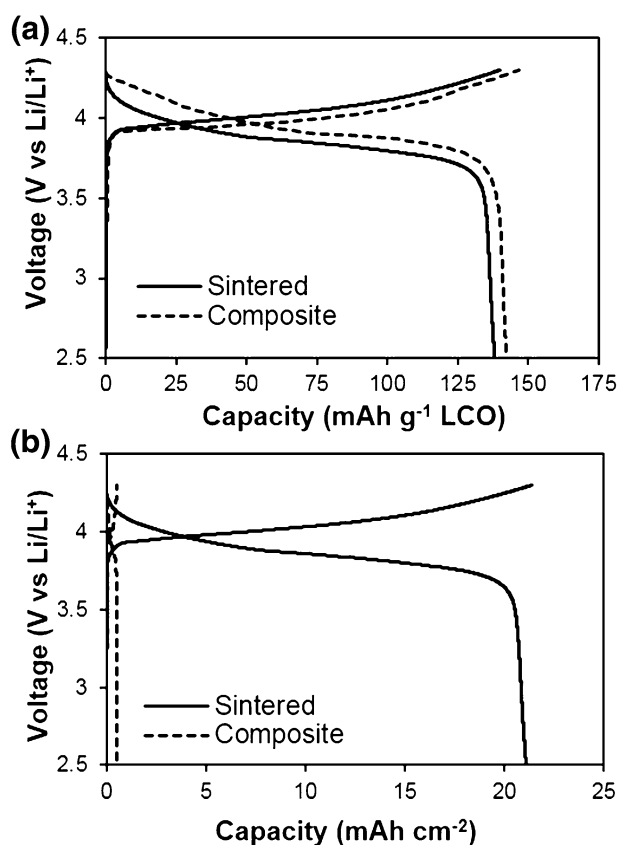


Fig. 1 Voltage profiles during charge/discharge for the 2nd cycle of sintered electrode (solid lines) and composite electrode (dashed lines) Li/LCO cells plotted on a **a** gravimetric basis considering just the active material and **b** areal basis. Areal current densities were 1.15 mA cm⁻² for the sintered electrode and 0.028 mA cm⁻² for the composite electrode, which for both cells corresponded to C/20 using a mass of active material basis

have only slightly lower capacity than the composites on a gravimetric basis, but much higher capacity on an areal basis. At C/20 (7.5 mA g⁻¹ LCO), the capacity of the sintered LCO electrode was 97% that of the composite LCO electrode on a gravimetric basis, but 4000% of the composite electrode on an areal basis. The round trip energy efficiency was 93.4% for the sintered electrode and 94.4% for the composite electrode. The volumetric energy density of the Li/LCO cell with the sintered electrode was calculated for just the active components of the cell and was very high – 1435 Wh L⁻¹ when discharged at a rate of 77.9 W L⁻¹. Note that the full 100 μm thick lithium metal anode, 400 μm thick LCO cathode with 68 vol% solid active material, electrolyte, and separator were included in this energy density, but the current collectors and cell casing were not included.

While the energy density of the Li/LCO cell with a sintered LCO electrode was very high, the cycle life was limited (Fig. 2a). The cell experienced abrupt capacity loss after 15 charge/discharge cycles at C/20. This low cycle life

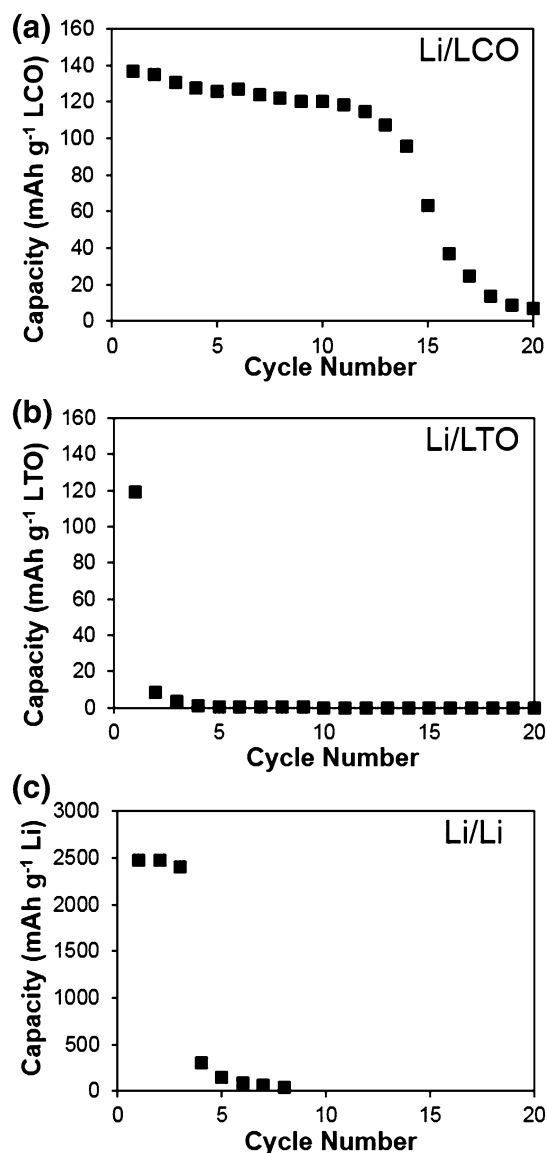


Fig. 2 Capacity retention during charge/discharge cycling of **a** Li/LCO and **b** Li/LTO cells containing sintered electrodes and **c** a Li/Li symmetric cell. The cells in **a** and **b** were cycled at rates corresponding to C/20 based on active material mass (areal current densities of 1.15 mA cm⁻² for LCO, 1.10 mA cm⁻² for LTO), while the cell in **c** was cycled using a 50 h cutoff for each charge/discharge at a rate of 0.53 mA cm⁻², which corresponded to C/50 for the sintered electrodes. Lithium metal mass for gravimetric basis in **c** corresponded to the mass of two layers of 100 μm lithium foil

made accurate determination of the rate capability of the sintered electrodes difficult. We hypothesized that the low cycle life was caused by the extremely deep lithium stripping and plating with each discharge and charge cycle, respectively. For example, assuming the lithium were to form a dense film with the reversible stripping and plating cycles, the early discharge cycles shown in Fig. 2a correspond to stripping a thickness of approximately 130 μm of lithium

metal during each cycle. That same approximately 130 μm of lithium metal would then be plated on the charge cycle. This substantial restructuring of the lithium anode with each cycle would be expected to result in large amounts of solid electrolyte interphase (SEI) formation and thus electrolyte consumption, as well as potential dendrite growth [20]. In a previous literature report characterizing sintered electrode cathodes, lithium metal and electrolyte were replaced periodically to enable extended cycling [4]. The challenge with extended cycling is expected to generally be an issue in thick sintered electrode cells when paired with lithium metal because of their high areal energy density, which is not an issue typically observed with lithium metal anode coin cells when paired with composite cathodes. This is because composite cathodes typically have only a couple mAh cm^{-2} capacity (e.g., Fig. 1b) and can be paired with lithium metal anodes that may be 200 μm thick, in which case assuming the lithium metal is a dense thin film, it would contain 41 mAh cm^{-2} of capacity. Thus, even with significant loss of lithium metal due to loss to SEI formation, because there are only a couple mAh of capacity on the cathode, the cells usually do not have problems reaching hundreds of charge/discharge cycles. However, for the sintered electrodes in this study, the cathode contains $> 20 \text{ mAh}$ —thus the cathode capacity goes from being $\sim 5\%$ of the lithium metal anode for the conventional composite electrode case to $\sim 50\%$ of the lithium metal anode in the sintered electrode case. Thus the lithium metal has to contend with extremely large swings in thickness with each cycle of stripping/plating and there is new SEI formation with each cycle. These combined factors are likely the cause of the relatively low number of cycles the sintered LCO electrode achieved when paired with lithium metal anodes.

As an alternative to using lithium metal as the anode, sintered $\text{Li}_4\text{Ti}_5\text{O}_{12}$ (LTO) spinel was investigated in an effort to achieve extended cycling without resorting to opening the cell and periodically replacing the electrolyte and lithium metal. LTO was chosen as the material for the anode material due to its 1.55 V redox potential vs. Li/Li^+ , which is within the stability window of the electrolyte and thus limits SEI formation. Though the higher redox potential reduces the energy density of Li-ion batteries with LTO relative to lithium metal or graphite anodes, the higher potential results in LTO having high cycle life and safety. Also, LTO has very low strain during intercalation/deintercalation, suppressing particle fracture during cycling [21, 22]. Additionally, while LTO as synthesized is initially electrically insulating, the $\text{Li}_7\text{Ti}_5\text{O}_{12}$ phase formed during lithiation is highly conductive and has been shown to support cycling LTO without carbon additives in both composite and sintered electrodes [23–25].

Since LTO has a low strain and the voltage is within the electrolyte stability window, it was expected to have high

retention of electrochemical capacity with charge/discharge when processed into a sintered electrode due to minimization of pulverization of interparticle connections which would enable maintaining conductivity throughout the thin film. However, despite these material stability advantages, sintered LTO electrodes paired with lithium metal anodes were observed to have even lower cycle life than sintered LCO electrodes (Fig. 2b). The Li/LTO cell with a sintered LTO electrode successfully completed one discharge/charge cycle at C/20 (see Fig. S2 in the Supplementary Material for the voltage profiles), but lost over 90% of cell capacity with the second discharge cycle. Capacity losses were always seen following delithiation of LTO (plating of lithium)—there were not significant losses following the lithiation of LTO (stripping of lithium) discharge cycle. Note that the thickness of lithium was doubled in Li/LTO cells to compensate for the initial discharge/lithiation reaction of LTO, as opposed to initial charge/delithiation reaction in Li/LCO cells (e.g., LCO starts on charge and thus there is more total lithium available for charge/discharge in a LCO vs. LTO electrode of equal capacity paired with an equivalent lithium metal anode). While it was surprising that the extra lithium metal thickness did not accommodate additional cycling for the LTO sintered electrode, again we suspect that the significant thickness change of the lithium metal electrode with cycling and additional SEI formation on the lithium during the extensive plating and stripping facilitated the dramatic capacity loss in the cell after the first charge/discharge cycle.

To further confirm the limitations of the lithium metal electrode in these high capacity cells, Li/Li symmetric cells were constructed using lithium foils with thickness of 200 μm (two 100 μm Li foils pressed together for each electrode) and electrode areas of 1.60 cm^2 . The Li/Li symmetric cell was unable to complete full 20 h cycles at current densities of $\sim 1.1 \text{ mA cm}^{-2}$, which corresponded to the current density used for C/20 cycling for the sintered electrodes, without hitting the 1.0 V upper voltage cutoff. To demonstrate cycling of the Li/Li cell, a current density of 0.53 mA cm^{-2} ($\sim \text{C}/50$ for sintered electrodes) was used and each cycle was set with a 50 h time cutoff for charge/discharge (Fig. 2c). Only three full “charge” and “discharge” cycles were achieved before loss of capacity in the Li/Li cell (charge and discharge in the symmetric cell refers to a switch in the electrode that was undergoing stripping or plating). While only the first eight discharge cycle data points are shown in Fig. 2c, there was negligible capacity delivered in the cell after the 8th cycle. The relatively large fraction of lithium metal stripped and plated with each cycle ($\sim 70\%$ of the initial lithium metal in the cell) would lead to significant SEI formation and loss of electrochemically accessible lithium in the cell. A voltage profile of the Li/Li cell is available in Fig. S3 in the Supplementary Material. While at 0.53 mA cm^{-2} , there was polarization in the Li/

Li cell that increased as a function of time both on charge and discharge, cycling at higher rates of $\sim 1.1 \text{ mA cm}^{-2}$ to $\sim 4.4 \text{ mA cm}^{-2}$ (corresponding to C/20 and C/5 for the sintered electrodes) resulted in very high polarization and the cell reaching the voltage cutoff of 1.0 V. The inability of the lithium metal to cycle at current densities that for the sintered electrodes corresponded to C/20 or higher presented a challenge in attempting to determine rate capability of the sintered electrode materials when paired with dense thin film lithium metal anodes.

2.2 Sintered electrode full cells

Due to the cycle life, capacity, and rate limitations of both the LCO and LTO sintered electrodes when paired with lithium metal, full cells were constructed to characterize the electrochemical performance of these electrodes without the use of lithium metal. LTO/LCO sintered electrode full cells of two different thicknesses were assembled and underwent galvanostatic cycling at various rates shown in Fig. 3. The difference between the data in Fig. 3a–d was the thickness and total amount of active material in the cell. The cell that provided the profiles and delivered capacities in Fig. 3c, d contained significantly thicker electrodes, although the

particles used to fabricate the electrodes and the sintering conditions were identical to the cell with thinner electrodes.

The cell shown in Fig. 3a, b contained an LTO-sintered electrode which was 0.75 mm thick and an LCO-sintered electrode which was 0.44 mm thick, for a total thickness for the electrodes and the separator of 1.21 mm. The LTO/LCO full cell achieved a capacity of 12.5 mAh cm^{-2} at the high current density of 4.62 mA cm^{-2} , and a capacity of 21.4 mAh cm^{-2} at the lowest evaluated current density of 0.462 mA cm^{-2} . The full cell was designed to be cathode limited in capacity and the LCO active material loading was 153 mg cm^{-2} —around six times higher than typical heavily loaded commercial composite electrodes [2, 18]. Although the cell was designed to be cathode limited, this was based on the capacity of the active materials when evaluated in composite electrodes, and because the Li/LTO-sintered electrode was difficult to evaluate, it is noted that it was possible that the sintered LTO electrode limited the discharge capacity in the cell. Detailed investigations determining the rate capability limitations of the LTO/LCO cells will be the subject of future investigations, but the thickness of these electrodes likely leads to significant concentration polarization and Li^+ diffusion limitations within the porous active material matrix, thus improvement of rate capability of these

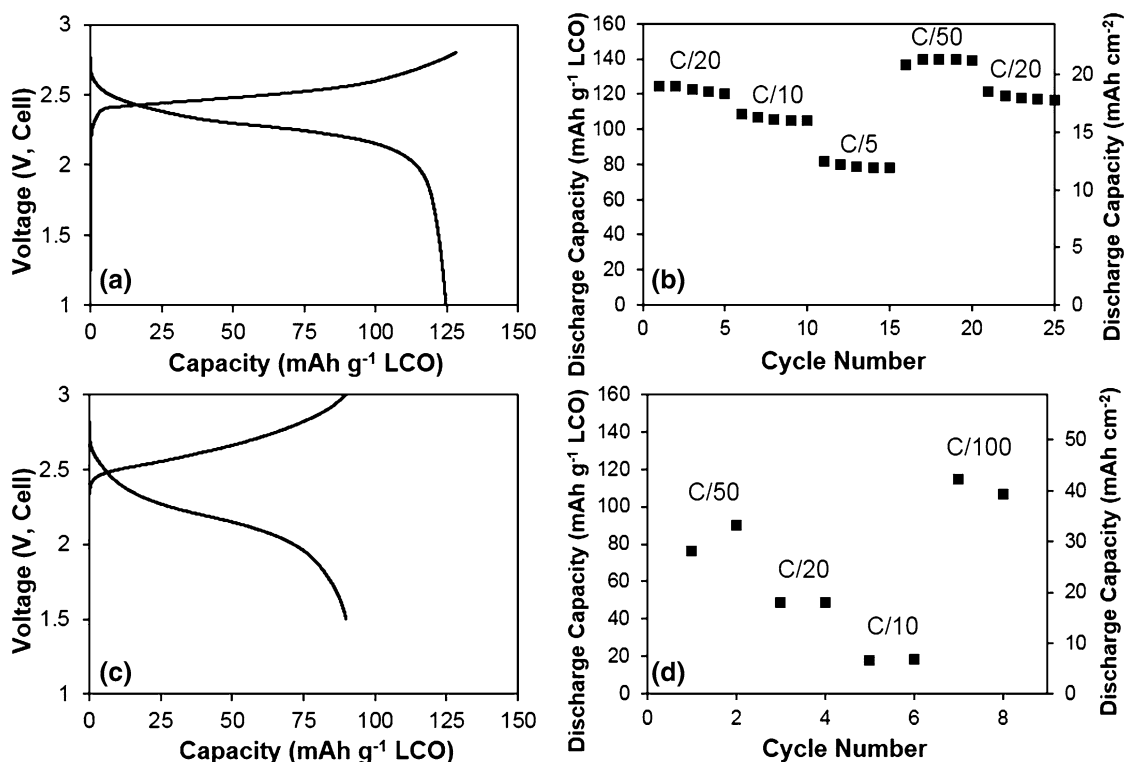


Fig. 3 a, c Voltage profiles for the 2nd charge/discharge cycle at C/20 and b, d rate capability of LTO/LCO cells where both the LTO and LCO were sintered electrodes. The cell in a, b contained a total anode, separator, and cathode thickness of 1.21 mm, while the cell

in c, d contained a total anode, separator, and cathode thickness of 2.90 mm. The profile in a had a voltage window of 1–2.8 V and areal current density of 1.15 mA cm^{-2} , while the cell in c had a voltage window of 1.5–3.0 V and areal current density of 1.36 mA cm^{-2}

electrodes will require careful design of the constituent particles, the Li^+ diffusion pathways, and the total electrode thickness [8]. Scanning electron micrographs of the films are available in Fig. S1 in the Supplementary Material.

To determine the electrochemical performance of much thicker sintered electrodes, a 2032-type coin cell was assembled with 2.90 mm total electrode and separator thickness (Fig. 3c, d). This combined thickness for the electrodes and separator was at the limit of what the 2032-type cell could accommodate. In order to fit the 1.08 mm thick LCO and 1.79 mm thick LTO electrodes, it was necessary to remove the spacers and wave spring, with the cell crimping providing the pressure in the cell which kept the electrodes in contact with the cell casing that provided the function of the current collectors. A relatively high voltage cutoff of 3.0 V (cell, vs. LTO anode) was used to extract additional capacity relative to the other LTO/LCO sintered electrode full cells, although such a high potential for LTO/LCO cells negatively impacts capacity retention. As seen in Fig. 3d, the cell delivered comparable gravimetric capacity on an LCO material basis to the 1.21 mm total thickness cell at low current densities. The theoretical capacity for the 2.90 mm thick cell was 109 mAh (based on 150 mAh g^{-1} LCO), and the highest discharge capacity achieved was 83.4 mAh at 1.28 mA cm^{-2} (C/100, the slowest rate used). With some optimization, a capacity of 120 mAh could reasonably be achieved in this cell geometry at the slower rates typical of many coin cell applications, and with an average voltage of around 2.5 V, this design compares favorably in energy density to rechargeable commercial coin cells such as ML2032 cells with approximately 2.5 V operating voltage and 65 mAh nominal capacity [26]. Furthermore, the cell still provides significant capacity even at a constant current discharge as high as 12.8 mA constant current, corresponding to the nominal C/10 discharge shown in Fig. 3d.

The capacity retention and rate capability of the 1.21 mm LTO/LCO full cell was greater than that of either the Li/LCO or Li/LTO cells, providing additional evidence that cycling and rate capability limitations in the Li/LTO and Li/LCO cells were likely due to the lithium metal electrodes rather than the sintered electrodes. The 1.21 mm thick cell retained 90.6% after 50 cycles and 85.3% after 200 cycles relative to the first cycle discharge capacity (see Supplementary Material, Fig. S4). Sintered electrodes have a unique reliance on small interparticle connections for connectivity and electronic conductivity. Due to the well-known issue of lithium intercalation and deintercalation causing strain and pulverization of active materials, it is expected that sintered electrodes will likely be more vulnerable than composites to intercalation pulverization. The low strain and high anode-side voltage of LTO make it one of the most durable Li-ion materials in composite cells, and it is expected that these properties are just as important for the sintered electrode

architecture. The mechanisms of capacity loss in sintered electrodes will be a topic for future studies; however, the results presented here demonstrate that high energy densities are made possible by using sintered electrodes comprised of only Li-ion battery active material as cell anodes and cathodes.

3 Conclusions

Li/LCO, Li/LTO, and LTO/LCO cells with thick and dense sintered electrodes have been fabricated and characterized through galvanostatic cycling. The cells containing lithium metal anodes have very high energy density; however, the cycle life of those cells was limited to as little as 1 charge/discharge cycle for Li/LTO, and these cycle life limitations were attributed to the lithium metal anode's inability to accommodate the high current densities and total capacities that result from using thick sintered electrodes. LTO/LCO full cells were assembled that had improved cycle life and rate capability relative to Li/LCO and Li/LTO cells, demonstrating that the short cycle life of the half cells was likely due to the deep cycling of lithium as opposed to pulverization of interparticle connections and loss of electronic conductivity and cohesion from the sintered electrodes. Additionally, reversible electrochemical cycling was demonstrated in a cell containing sintered electrodes for both the anode and cathode and a total electrode and separator thickness up to 2.90 mm, resulting in extremely high areal loadings and areal capacities. Further efforts will be needed to probe capacity loss mechanisms within sintered electrode films, as well as further optimization of the sintered electrode particle constituents and microstructures to improve these unique battery electrode materials.

4 Experimental

4.1 Preparation of active material powders

LCO was synthesized using an adapted method previously reported in the literature [27]. First, $\text{CoC}_2\text{O}_4 \cdot 2\text{H}_2\text{O}$ precipitate particles were synthesized by pouring all at once an 1800 mL solution of 62.8 mM $\text{Co}(\text{NO}_3)_2 \cdot 6\text{H}_2\text{O}$ (Fisher Reagent Grade) dissolved in deionized (DI) water into an 1800 mL solution of 87.9 mM $(\text{NH}_4)_2\text{C}_2\text{O}_4 \cdot \text{H}_2\text{O}$ (Fisher Certified ACS) dissolved in DI water. Solutions were preheated to 50 °C prior to mixing and the temperature was maintained at 50 °C for the duration of the synthesis. The solution was stirred continuously and vigorously at 800 rpm with a magnetic stirrer. After 30 min of precipitation, $\text{CoC}_2\text{O}_4 \cdot 2\text{H}_2\text{O}$ particles were collected via vacuum filtration, rinsed with 4 L of DI water, and vacuum dried overnight at 80 °C.

$\text{CoC}_2\text{O}_4 \cdot 2\text{H}_2\text{O}$ powder was mixed with Li_2CO_3 (Fisher Certified ACS) powder with 2% excess Li salt relative to stoichiometric quantities (e.g.; Li:Co mixed at 1.02:1 molar ratio) in a mortar and pestle. The mixed powder was fired at a 1°C per minute ramp rate to 800°C with no hold time in a Carbolite CWF 1300 box furnace in air, and upon reaching 800°C the furnace was turned off and allowed to cool to ambient temperature without control over cooling rate. After firing, the resulting LCO powder was milled in a Fritsch Pulverisette 7 planetary ball mill with 5 mm diameter zirconia beads for 5 h at 300 rpm.

The LTO powder used was NANOMYTE BE-10 purchased from NEI Corporation. Characterization of this material can be found in previous reports [28].

4.2 Electrode preparation and characterization

Active material powder was mixed with solution containing 1 wt% polyvinyl butyral dissolved in ethanol at a ratio of 2 mL binder solution:1 g active material powder using a mortar and pestle. After solvent evaporation by exposure to air, the active material and binder mixture was further ground in a mortar and pestle. Either 0.2 g LCO-binder mixture or 0.22 g LTO-binder mixture were loaded into a 13 mm diameter Carver pellet die and pressed with 12,000 lb_f for 2 min in a Carver hydraulic press. A 16 mm diameter pellet die was used for the very thick LCO and LTO electrodes (Fig. 3c, d). After pressing, electrodes were sintered in a Carbolite CWF 1300 box furnace in air through heating to a peak temperature of 700°C and held for 1 h with a 1°C per minute ramping and cooling rate. After cooling, electrodes were attached directly to stainless steel coin cell spacers using an *N*-methyl pyrrolidone (NMP) solvated binder slurry of 1:1 weight ratio Super P carbon black conductive additive to polyvinylidene difluoride (PVDF) binder and dried overnight in an 80°C oven.

Composite electrodes were prepared by coating a slurry comprised of active material (for LTO directly as received, for LCO after ball milling), carbon black conductive additive, and PVDF binder in NMP solvent with a weight ratio of 80:10:10 active:carbon black:PVDF onto an aluminum foil current collector using a doctor blade with a gap of 200 μm . The electrode slurry was dried in an 80°C oven overnight and dried in an 80°C vacuum oven for 3 h prior to punching out 14 mm diameter electrode disks.

Electrodes for all cells were assembled into CR2032 coin cells in an argon atmosphere glove box with a single trilayer polymer separator and an electrolyte comprised of 1.2 M LiPF_6 in 3:7 ethylene carbonate:ethyl methyl carbonate electrolyte. Cells were tested through constant current charge/discharge cycling on a MACCOR battery cyler. Where reported, C rates were based on assumed capacities of 150 mAh g^{-1} for LCO and 175 mAh g^{-1}

for LTO (e.g., 1C for LCO electrodes was 150 mA g^{-1} LCO). Voltage ranges and current densities used during cell cycling for different cell types (Li/LTO, Li/LCO, LTO/LCO with sintered or composite electrodes and different loadings) can be found in the text and figure captions for each cell discussed.

Acknowledgements This research was supported by the National Science Foundation through award ECCS-1405134 and by the 4-VA program in Virginia.

References

1. Nitta N, Wu F, Lee JT, Yushin G (2015) Li-ion battery materials: present and future. *Mater Today* 18:252–264. <https://doi.org/10.1016/j.mattod.2014.10.040>
2. Andre D, Kim S-J, Lamp P et al (2015) Future generations of cathode materials: an automotive industry perspective. *J Mater Chem A* 3:6709–6732. <https://doi.org/10.1039/C5TA00361J>
3. Qi Z, Koenig GM (2017) Review article: flow battery systems with solid electroactive materials. *J Vac Sci Technol B* 35:40801. <https://doi.org/10.1116/1.4983210>
4. Lai W, Erdonmez CK, Marini TF et al (2010) Ultrahigh-energy-density microbatteries enabled by new electrode architecture and micropackaging design. *Adv Mater* 22:139–144
5. Ning H, Pikul JH, Zhang R et al (2015) Holographic patterning of high-performance on-chip 3D lithium-ion microbatteries. *Proc Natl Acad Sci* 112:6573–6578. <https://doi.org/10.1073/pnas.1423889112>
6. Chen Z, Dahn JR (2002) Reducing carbon in LiFePO_4 /C composite electrodes to maximize specific energy, volumetric energy, and tap density. *J Electrochem Soc* 149:A1184. <https://doi.org/10.1149/1.1498255>
7. Chen J, Liu J, Qi Y et al (2013) Unveiling the roles of binder in the mechanical integrity of electrodes for lithium-ion batteries. *J Electrochem Soc* 160:A1502–A1509. <https://doi.org/10.1149/2.088309jes>
8. Singh M, Kaiser J, Hahn H (2015) Thick electrodes for high energy lithium ion batteries. *J Electrochem Soc* 162:A1196–A1201. <https://doi.org/10.1149/2.0401507jes>
9. Kitada K, Murayama H, Fukuda K et al (2016) Factors determining the packing-limitation of active materials in the composite electrode of lithium-ion batteries. *J Power Sources* 301:11–17. <https://doi.org/10.1016/j.jpowsour.2015.09.105>
10. Wood DL, Li J, Daniel C (2015) Prospects for reducing the processing cost of lithium ion batteries. *J Power Sources* 275:234–242. <https://doi.org/10.1016/j.jpowsour.2014.11.019>
11. Srinivasan V, Newman J (2004) Discharge model for the lithium iron-phosphate electrode. *J Electrochem Soc* 151:A1517. <https://doi.org/10.1149/1.1785012>
12. Chung D-W, Shearing PR, Brandon NP et al (2014) Particle size polydispersity in Li-ion batteries. *J Electrochem Soc* 161:A422–A430. <https://doi.org/10.1149/2.097403jes>
13. Zheng H, Li J, Song X et al (2012) A comprehensive understanding of electrode thickness effects on the electrochemical performances of Li-ion battery cathodes. *Electrochim Acta* 71:258–265. <https://doi.org/10.1016/j.electacta.2012.03.161>
14. Yang G-F, Song K-Y, Joo S-K (2015) Ultra-thick Li-ion battery electrodes using different cell size of metal foam current collectors. *RSC Adv* 5:16702–16706. <https://doi.org/10.1039/C4RA14485F>

15. Wang K-X, Li X-H, Chen J-S (2015) Surface and interface engineering of electrode materials for lithium-ion batteries. *Adv Mater* 27:527–545. <https://doi.org/10.1002/adma.201402962>
16. Bae CJ, Erdonmez CK, Halloran JW, Chiang YM (2013) Design of battery electrodes with dual-scale porosity to minimize tortuosity and maximize performance. *Adv Mater* 25:1254–1258. <https://doi.org/10.1002/adma.201204055>
17. Du Z, Wood DL, Daniel C et al (2017) Understanding limiting factors in thick electrode performance as applied to high energy density Li-ion batteries. *J Appl Electrochem* 47:405–415. <https://doi.org/10.1007/s10800-017-1047-4>
18. Marks T, Trussler S, Smith AJ et al (2011) A guide to Li-ion coin-cell electrode making for academic researchers. *J Electrochem Soc* 158:A51–A57. <https://doi.org/10.1149/1.3515072>
19. Levasseur S, Menetrier M, Delmas C (2002) On the dual effect of Mg doping in LiCoO_2 and $\text{Li}_1+\delta\text{CoO}_2$: structural, electronic properties, and Li-7 MAS NMR studies. *Chem Mater* 14:3584–3590. <https://doi.org/10.1021/cm021107j>
20. Wood KN, Noked M, Dasgupta NP (2017) Lithium metal anodes: toward an Improved understanding of coupled morphological, electrochemical, and mechanical behavior. *ACS Energy Lett* 2:664–672. <https://doi.org/10.1021/acseenergylett.6b00650>
21. Ohzuku T, Ueda A, Yamamoto N (1995) Zero-strain insertion material of $\text{Li Li}_{1/3}\text{Ti}_{5/3}\text{O}_4$ for rechargeable lithium cells. *J Electrochem Soc* 142:1431–1435. <https://doi.org/10.1149/1.2048592>
22. Yang Z, Choi D, Kerisit S et al (2009) Nanostructures and lithium electrochemical reactivity of lithium titanates and titanium oxides: a review. *J Power Sources* 192:588–598. <https://doi.org/10.1016/j.jpowsour.2009.02.038>
23. Kim C, Norberg NS, Alexander CT et al (2013) Mechanism of phase propagation during lithiation in carbon-free $\text{Li}_4\text{Ti}_5\text{O}_{12}$ battery electrodes. *Adv Funct Mater* 23:1214–1222. <https://doi.org/10.1002/adfm.201201684>
24. Song M-S, Benayad A, Choi Y-M, Park K-S (2012) Does $\text{Li}_4\text{Ti}_5\text{O}_{12}$ need carbon in lithium ion batteries? Carbon-free electrode with exceptionally high electrode capacity. *Chem Commun* 48:516–518. <https://doi.org/10.1039/C1CC16462G>
25. Young D, Ransil A, Amin R et al (2013) Electronic conductivity in the $\text{Li}_{4/3}\text{Ti}_{5/3}\text{O}_4\text{-Li}_{7/3}\text{Ti}_{5/3}\text{O}_4$ system and variation with state-of-charge as a Li battery anode. *Adv Energy Mater* 3:1125–1129. <https://doi.org/10.1002/aenm.201300134>
26. (2017) Maxell. http://biz.maxell.com/en/rechargeable_batteries/ML2032_DataSheet_17e.pdf
27. Qi Z, Koenig GM (2016) High-performance LiCoO_2 sub-micrometer materials from scalable microparticle template processing. *ChemistrySelect* 1:3992–3999. <https://doi.org/10.1002/slct.201600872>
28. Qi Z, Koenig GM (2016) A carbon-free lithium-ion solid dispersion redox couple with low viscosity for redox flow batteries. *J Power Sources* 323:97–106. <https://doi.org/10.1016/j.jpowsour.2016.05.033>